



Figures and figure supplements

The novel lncRNA *lnc-NR2F1* is pro-neurogenic and mutated in human neurodevelopmental disorders

Cheon Euong Ang et al

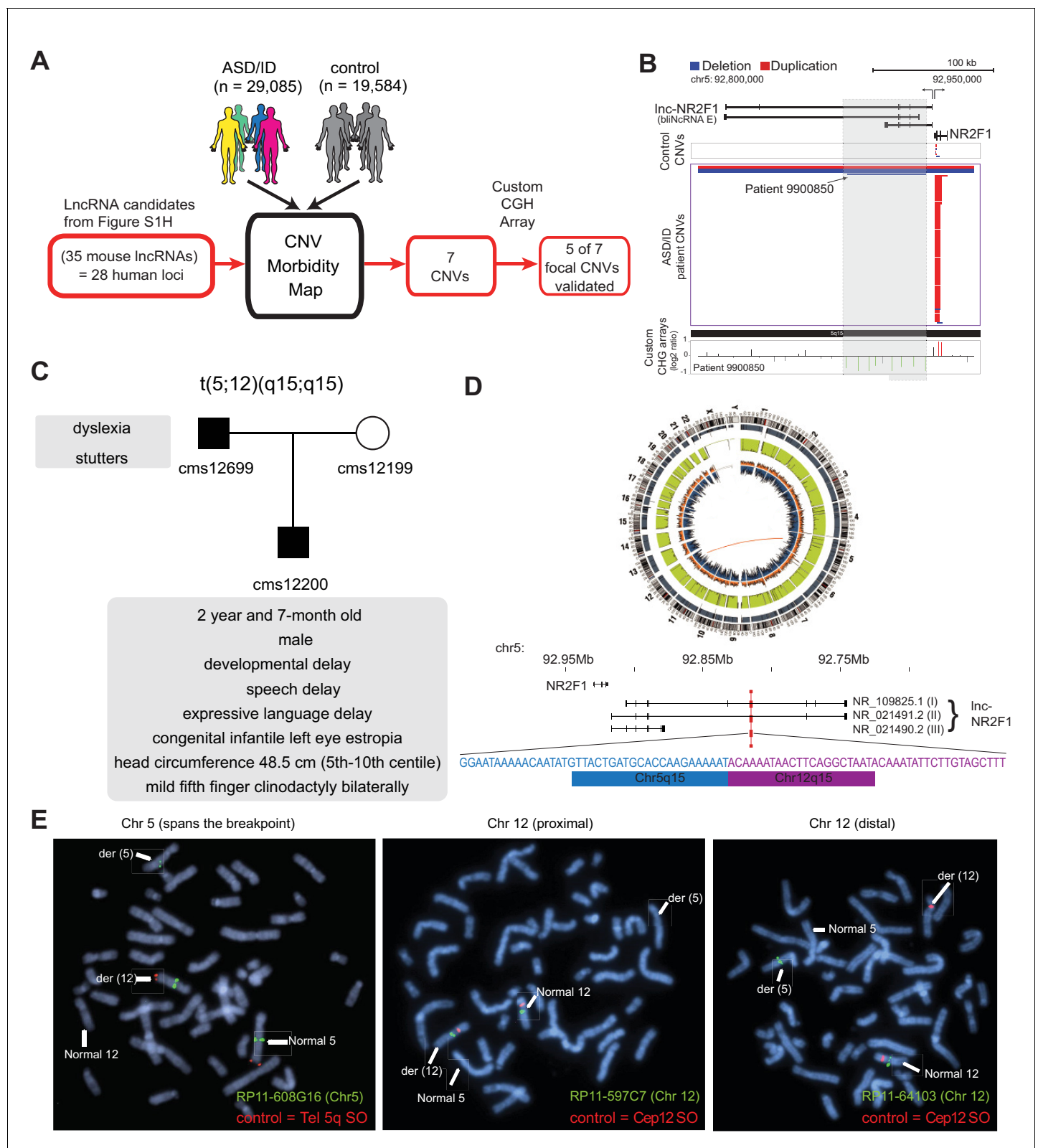


Figure 1. lncRNA loci are recurrently mutated in patients with neurodevelopmental disorders. (A) Schematic representation of CNV morbidity map analysis for candidate lncRNAs and all other iN lncRNAs loci. The 35 mouse lncRNA candidates (28 human loci) is from **Figure 1—figure supplement 1H**. (B) Top: Representative tracks for lncRNA E locus, also known as *Inc-NR2F1*. Depicted in blue are deletions and in red duplications. Arrow points to patient with focal deletion affecting the *Inc-NR2F1* locus only. Bottom: Custom CGH arrays used to validate chromosomal aberration in patient 9900850

Figure 1 continued on next page

Figure 1 continued

harboring focal deletion represented in green signal. (C) Genetic pedigree analysis for family with paternally inherited balanced chromosomal translocation (5;12) (q15;q15), including a summary of clinical features for patient CMS12200 and father. The mother has a normal karyotype. Listed in the box are the symptoms of the patients. (D) Top: Circa plot representing the pathogenic chromosomal event for patient CMS12200 involving chromosomes 5 and 12. Bottom: Representative chromosome ideogram and track of the balanced chromosomal break affecting patient CMS12200. Below the ideoplot is the schematic representation of predominant human isoforms for *Inc-NR2F1* and the site of the break site disrupting the long isoforms. (E) The locations of the probes are in **Figure 1—figure supplement 4C**. Left: Metaphase spread from patient CMS12200 with the t(5;12) translocation showing FISH signals obtained with the clone RP11-608G16 (green) spanning Chromosome five breakpoint, and a Chromosome five telomere-specific probe (red). Middle: Metaphase spread from patient CMS12200 with the t(5;12) translocation showing FISH signals obtained with the clone RP11-597C7(green) proximal to Chromosome 12 breakpoint, and a Chromosome 12 centromere-specific probe (red). Right: Metaphase spread from patient CMS12200 with the t(5;12) translocation showing FISH signals obtained with the clone RP11-641O3 (green) distal to Chromosome 12 breakpoint, and a Chromosome 12 centromere-specific probe (red).

DOI: <https://doi.org/10.7554/eLife.41770.002>

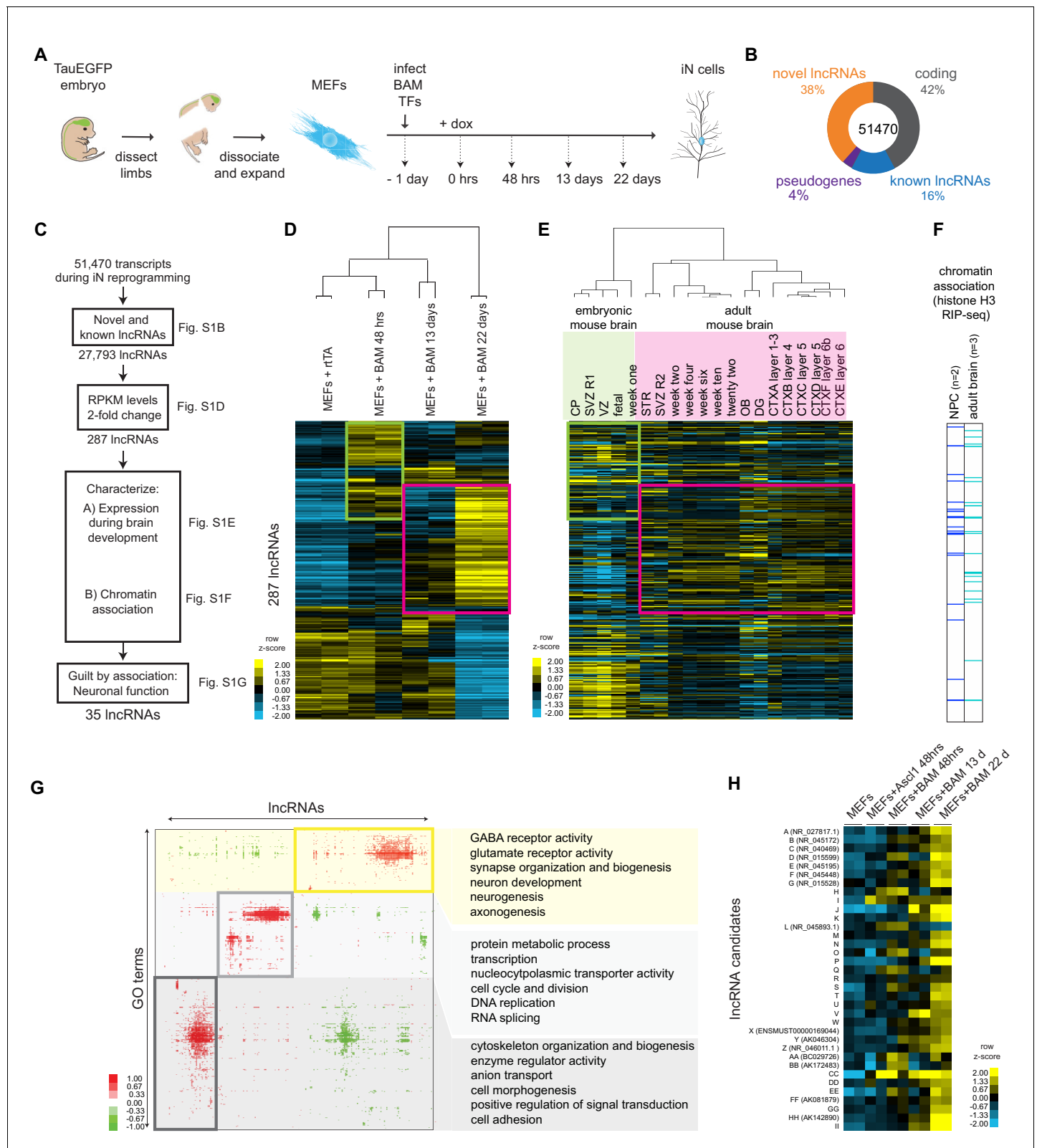


Figure 1—figure supplement 1. Molecular profiling of direct fibroblast to iN cell reprogramming nominates functional lncRNAs involved in neurogenesis. (A) Schematic representation of experimental time points generated for this study. (B) Classification of the iN cell transcriptome consisting of 51,470 transcripts based on coding genes and non-coding RNAs. (C) Diagram depicting pipeline derived in this study to enrich for candidate lncRNAs with strong neuronal association. (D) Hierarchical clustering heatmap of lncRNA expression during iN cell reprogramming by RNA-seq. Figure 1—figure supplement 1 continued on next page

Figure 1—figure supplement 1 continued

seq across indicated time points ($n = 2$ biological replicates). Shown are 287 lncRNAs that changed expression at least two-fold at any time point ($p < 0.05$). Fold change is represented in logarithmic scale normalized to the mean expression value of a gene across all samples. The green box highlights the genes which are upregulated in the MEF +BAM 48 hr. The same set of genes are upregulated in embryonic mouse brain (see **Figure 1—figure supplement 1E**). The pink box highlights the genes which are upregulated in the MEF +BAM 22 hr. The same set of genes are upregulated in adult mouse brain (see **Figure 1—figure supplement 1E**). (E) Hierarchical clustering heatmap of iN lncRNAs from **Figure 1—figure supplement 1D** across mouse brain tissues from publicly available data. Expression levels are represented in logarithmic scale normalized to the mean expression value of a gene across all samples. (F) Chromatin association of iN lncRNAs determined by histone H3-RIP-seq in Neuronal Progenitor Cells (NPCs) and total adult brain ($n = 2$ biological replicates for NPCs and $n = 3$ for mouse brain) presented in binary format. Shown are lncRNAs that have significant enrichment over background (>2 fold, $p < 0.05$) and consistent enriched in the chromatin among biological replicates. (G) Co-expression analysis using Genomica between iN lncRNAs and mRNAs associated with Gene ontology (GO) terms. Highlighted in the yellow box are lncRNA candidates which are associated with neuronal GO terms. (H) RNA-seq heatmap of 35 filtered candidate lncRNAs across MEF-to-iN cell reprogramming. In brackets are the Refseq ID for the annotated lncRNAs. See the supplementary documents for the sequences and coordinates of the 35 candidates.

DOI: <https://doi.org/10.7554/eLife.41770.003>

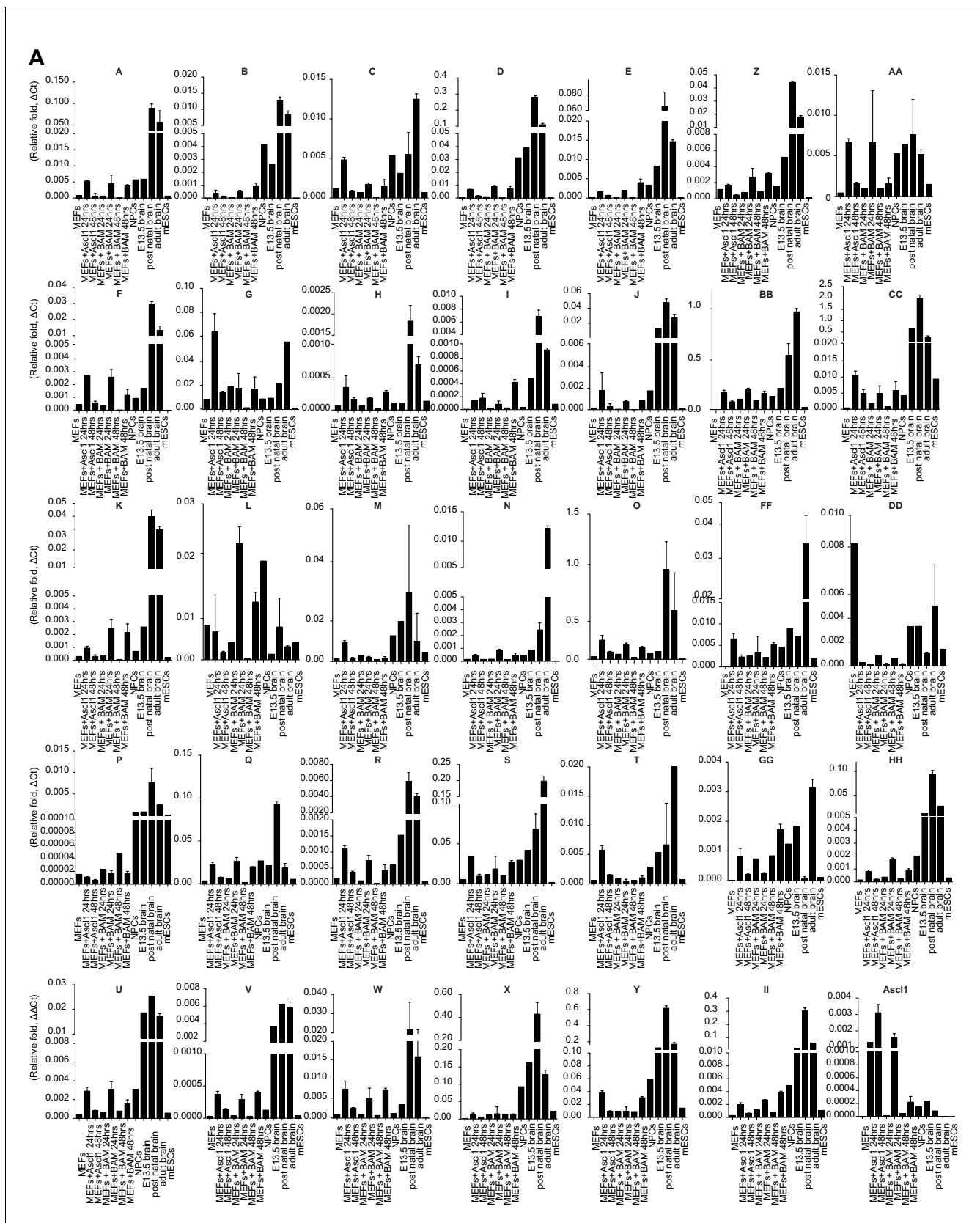


Figure 1—figure supplement 2. QRT-PCR validation of candidate lncRNAs expression. (A) Expression detection of candidate lncRNAs by qRT-PCR across early stages of iN cell reprogramming and mouse brain development.

DOI: <https://doi.org/10.7554/eLife.41770.004>

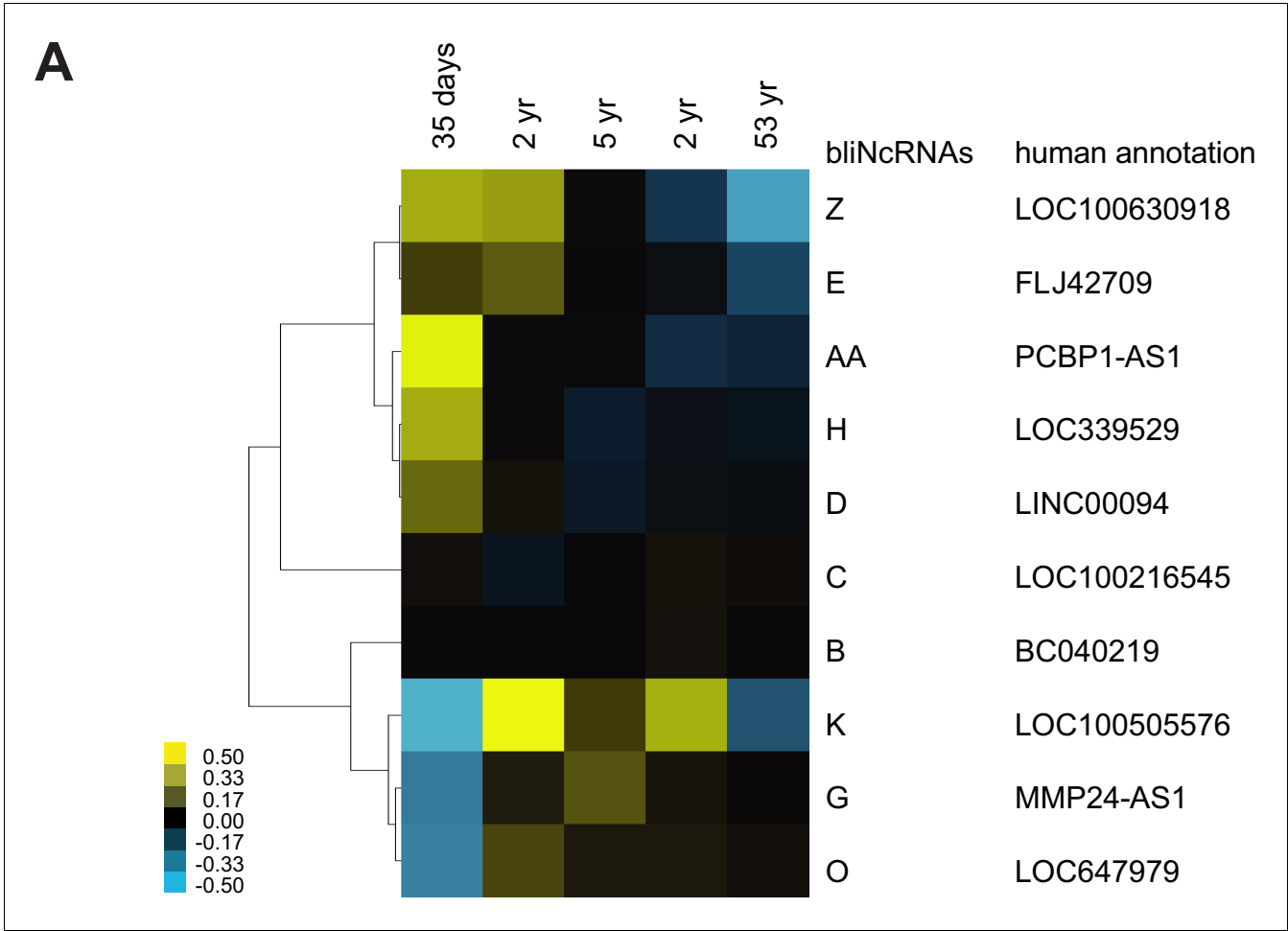


Figure 1—figure supplement 3. Conserved lncRNAs have distinct pattern of expression across different stages of the human brain. (A) Heatmap of annotated syntenic lncRNAs across human brain development detected by RNA-seq. Expression is represented in logarithmic scale normalized to the mean RPKM value of a gene across all samples. See Supplementary documents for the lncRNA sequences.
DOI: <https://doi.org/10.7554/eLife.41770.005>

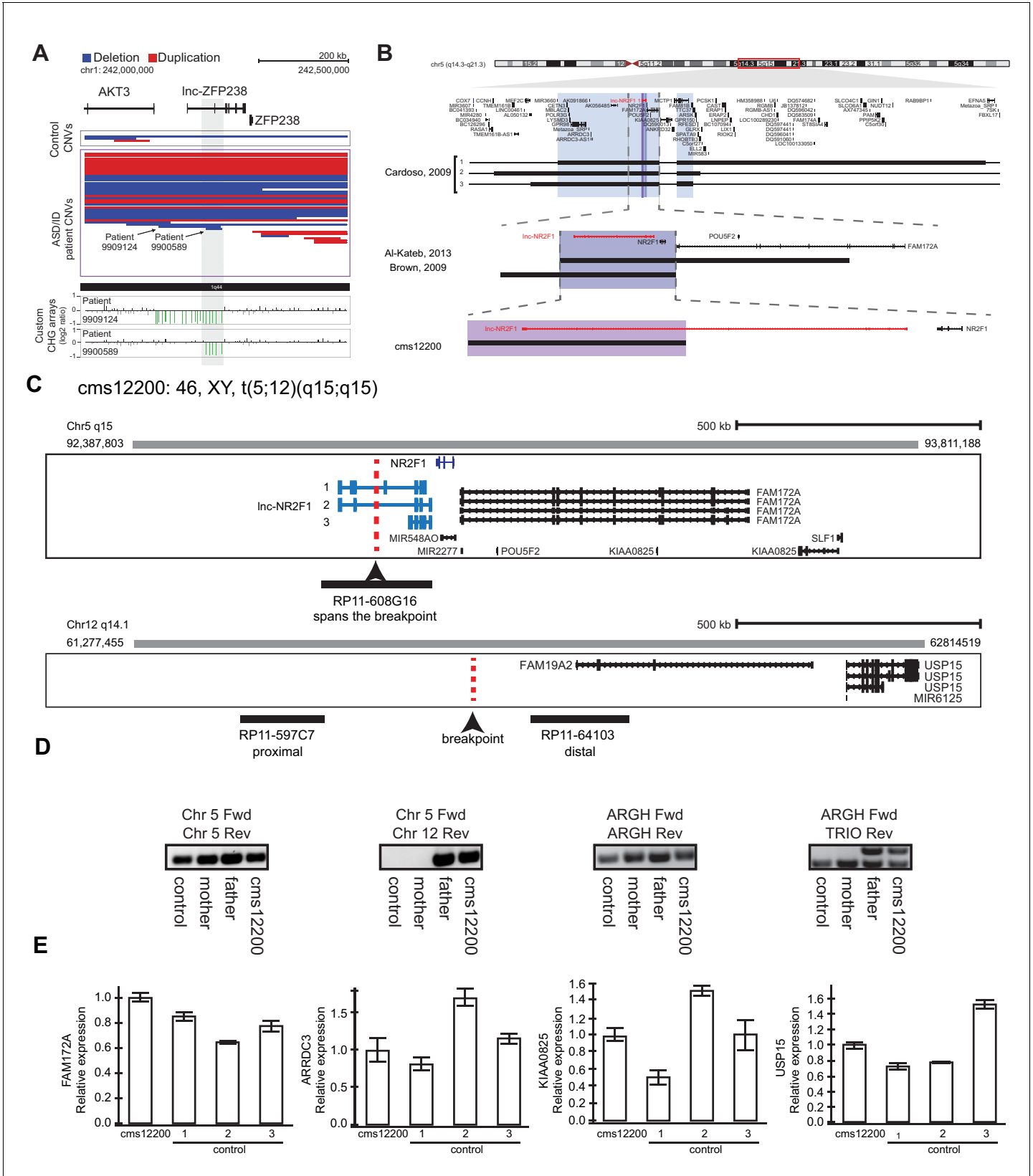


Figure 1—figure supplement 4. Other reports of CNVs affecting *Inc-NR2F1* and an example of focal deletion affecting *Inc-ZFP238* and characterization for patient CMS12200. (A) Top: Representative tracks for *IncRNA H* locus, also known as *Inc-ZFP238*. Depicted in blue are deletions and

Figure 1—figure supplement 4 continued on next page

Figure 1—figure supplement 4 continued

in red duplications. Arrow points to two significant focal deletions in two distinct patients. Bottom: Custom CGH arrays used to validate chromosomal aberration in patients 9909124 and 9900589 harboring focal deletions represented in green signal. (B) Representative tracks of previously reported deletions affecting chromosome region 5q15 in patients with neurodevelopmental and neuropsychiatric disorders. The black rectangle represents affected genomic region corresponding to the patient described in a previous publication to the left. Top panel: light blue box represents minimal common region amongst three patients in Cardoso et al, 2009 report. There are multiple genes affected in the locus. Middle panel: purple box depicts common deleted region reported amongst two patients from Brown, et al 2009, and Al-Kateb, et al 2013 studies. The region encompasses only two genes: *NR2F1* and *Inc-NR2F1*. Bottom panel: Patient CMS 12200 described in this study harboring a balanced chromosomal translocation disrupting *Inc-NR2F1* only as depicted by the pink box. In red, *Inc-NR2F1* is highlighted. (C) Schematic representation of breakpoint region between chromosome 5 and 12 for patient CMS12200. Illustrated is also the probe design to confirm event. Probe RP11-608G16 spans the breakpoint in chromosome 5. Probe RP11-597C7 is proximal to the breakpoint on chromosome 12. Probe RP11-64103 is distal to the breakpoint on chromosome 12. (D) Genomic PCR to confirm t(5;12) translocation using primers spanning control region in chromosome 5 (left), translocation between chromosome 5 and 12 (middle left), unaffected region in ARGH gene (middle right), and non-pathological gene duplication for TRIO exon in ARGH intronic loci (right). Samples from control (GM12878), mother (does not harbor translocation), father (t(5;12)), and CMS12200 patient (t(5;12)). (E) Expression of genes proximal to breakpoint is unaffected as measured by RT-qPCR in CMS12200 patient lymphocytes and three distinct control samples.

DOI: <https://doi.org/10.7554/eLife.41770.006>

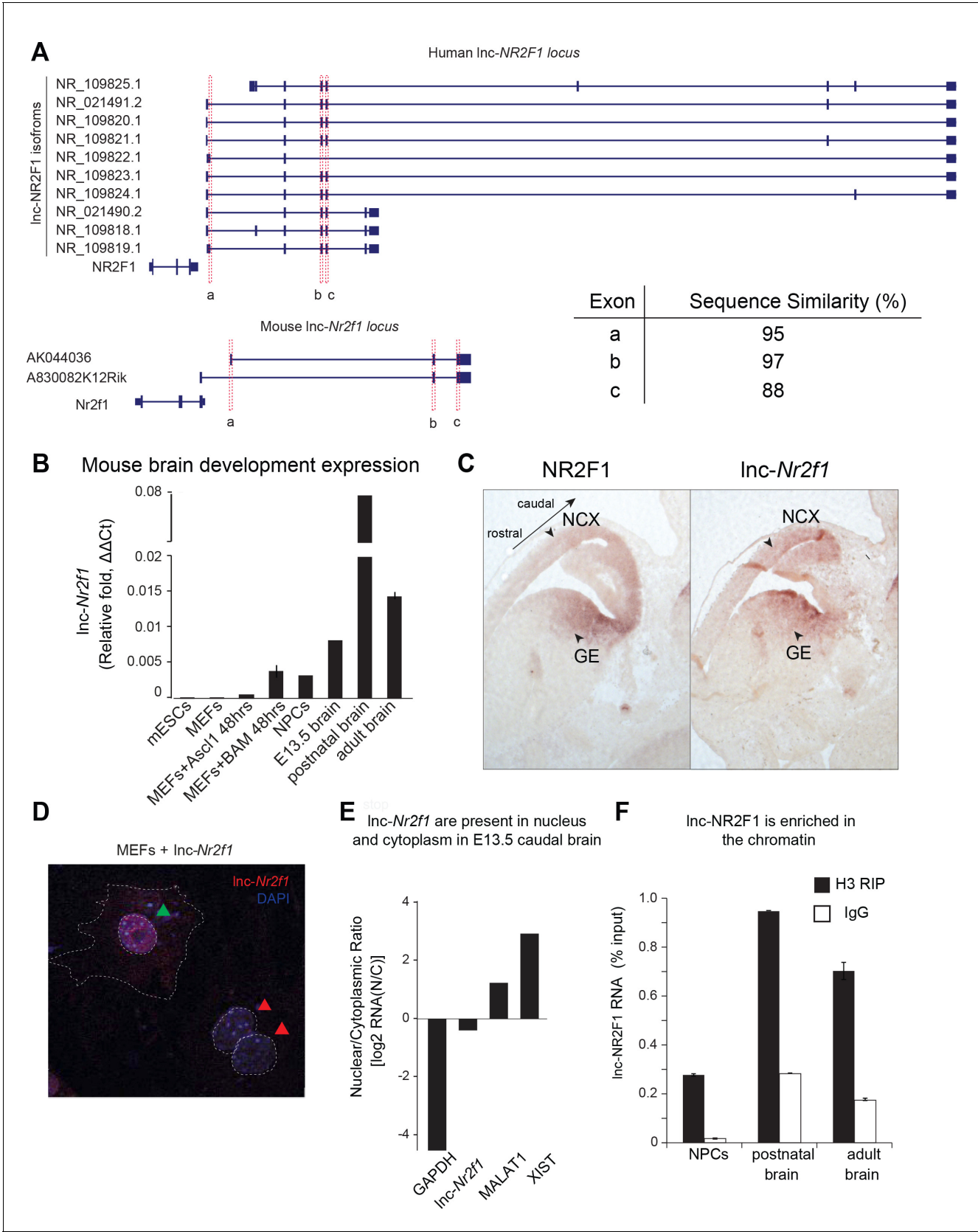


Figure 2. Molecular characterization of mouse *Inc-Nr2f1*. (A) Schematic showing the different isoforms reported by Refseq of the human *Inc-NR2F1* and mouse *Inc-Nr2f1*. Exons highlighted in red are conserved among human and mouse. The table at the bottom right corner shows the sequence similarity

Figure 2 continued on next page

Figure 2 continued

as reported by T-COFFEE. The sequence alignment is available as **Supplementary file 6**. (B) *Lnc-Nr2f1* expression measured by qRT-PCR across stages of mouse brain development and early stages of iN cell reprogramming. Results show early detection in E13.5 brain, peak expression at postnatal stages, and continued expression through adulthood. (C) In situ hybridization for *Nr2f1* and *Lnc-Nr2f1* shows similar expression pattern in E13.5 mouse brain. Highlighted by arrows are neocortex (NCX) and ganglionic eminences (GE) with high expression levels. (D) Cellular localization of *Lnc-Nr2f1* by single molecule RNA-FISH in MEFs ectopically expressing the lncRNA 48 hr after dox induction reveals nuclear and cytoplasmic localization, with slight nuclear enrichment. Green arrow points at *Lnc-Nr2f1* in the nucleus and red arrows point at the uninfected nuclei. (E) Cellular fractionation of primary neurons derived from E13.5 caudal cortex dissection shows nuclear and cytoplasmic localization of *Lnc-Nr2f1*. (F) Chromatin enrichment of *Lnc-Nr2f1* by histone H3 RIP-qRT-PCR in brain derived neuronal precursor cells (NPCs), postnatal and adult mouse brain.

DOI: <https://doi.org/10.7554/eLife.41770.007>

ANKRD32

Figure 2—figure supplement 1 continued

track showing the sequence conservation of the three exons (highlighted in red) across different species. (C) Sequences around the conserved exons show short sequence homology from different species. MEME (<http://meme-suite.org/tools/meme>) is used to discover motif homology. See Supplementary documents for the sequences used.

DOI: <https://doi.org/10.7554/eLife.41770.008>

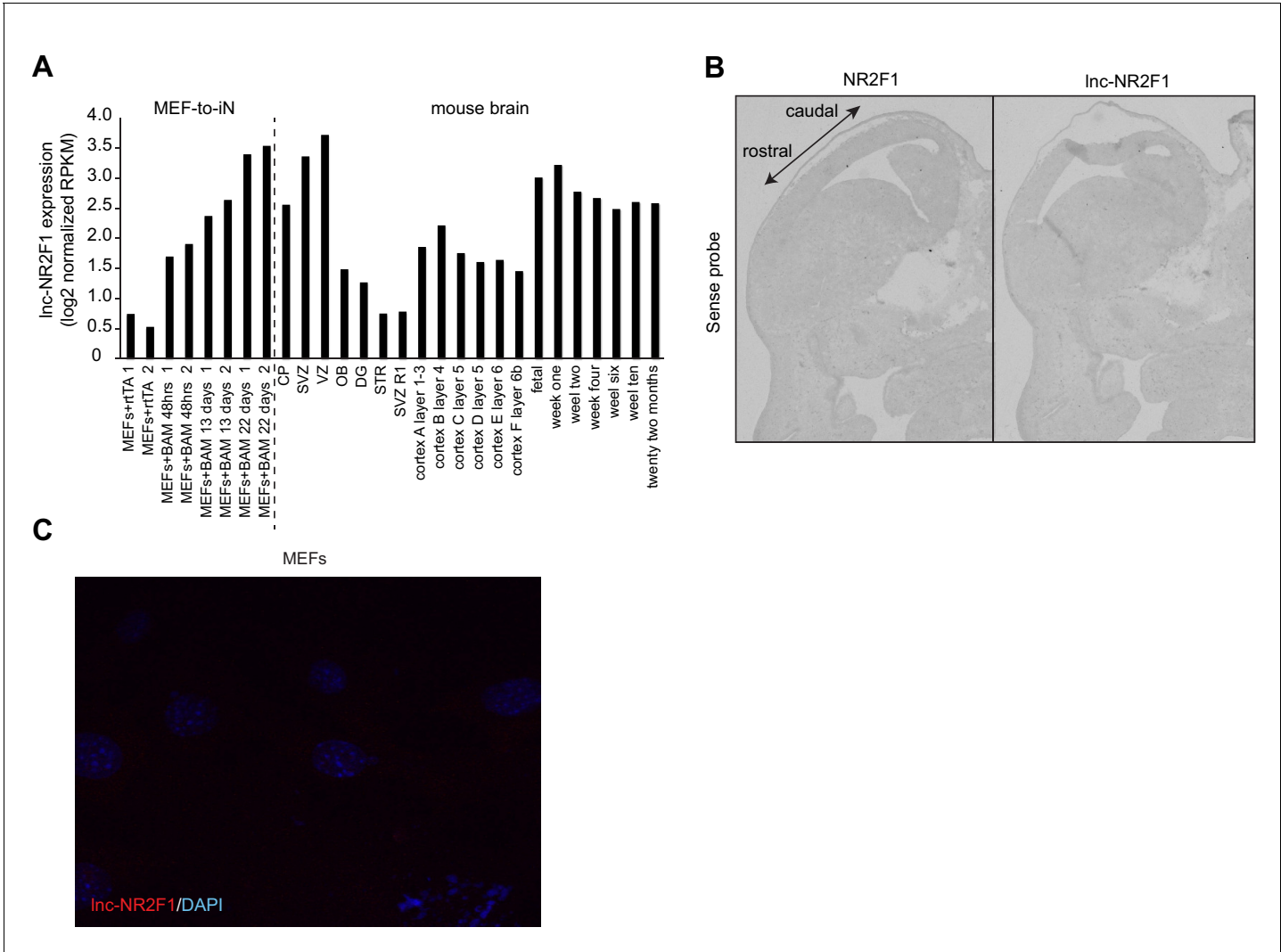


Figure 2—figure supplement 2. Characterization of *Inc-Nr2f1* localization. (A) RPKM counts for *Inc-Nr2f1* during MEF-to-iN-reprogramming and across different stages and tissues of mouse brain development. (B) Control in situ hybridization for NR2F1 and *Inc-Nr2f1* using sense probe. (C) Control single molecule RNA-FISH in MEFs infected with rtTA alone in order to determine background signal.

DOI: <https://doi.org/10.7554/eLife.41770.009>

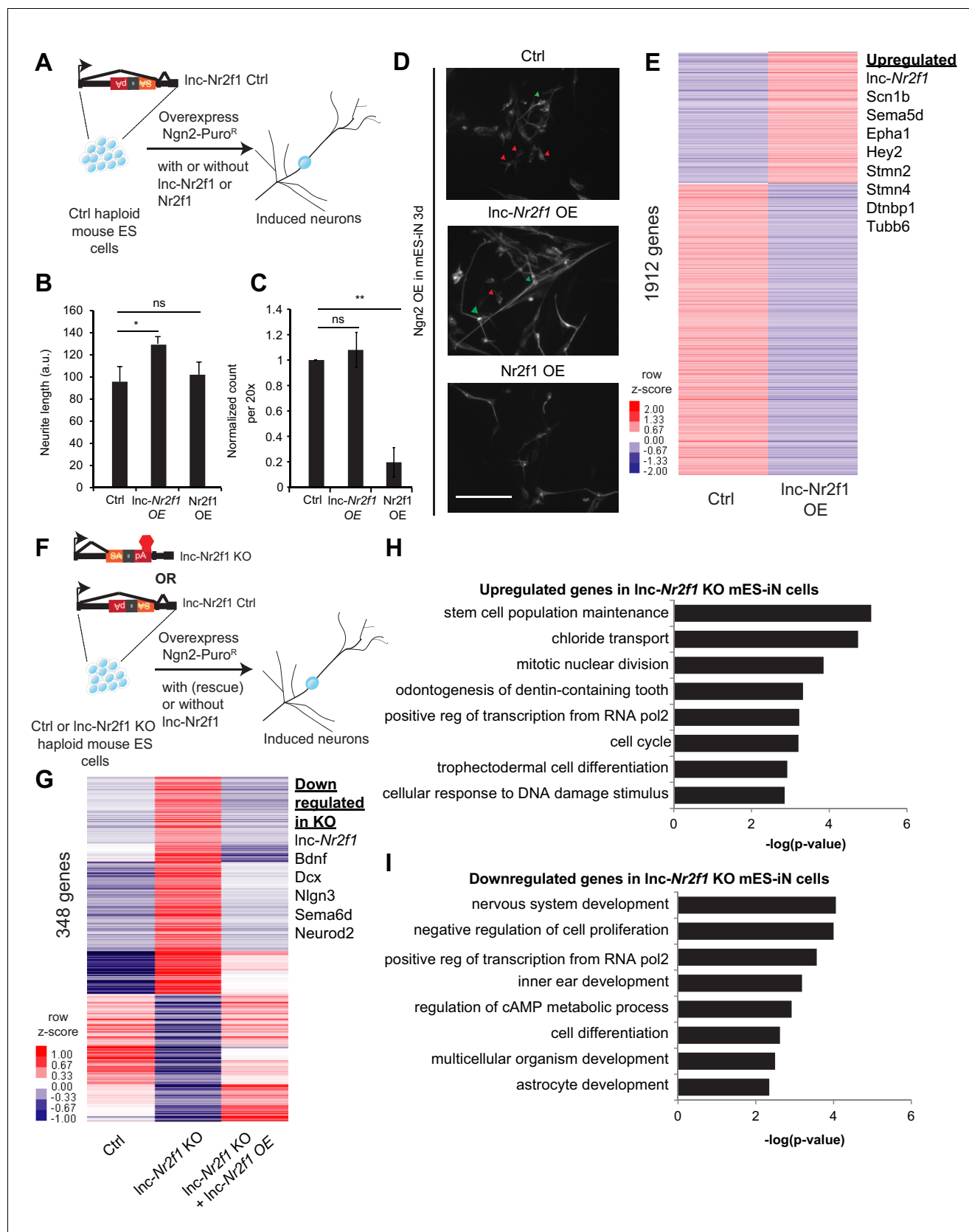


Figure 3. Mouse *Lnc-Nr2f1* KO reveals *Lnc-Nr2f1* regulates neuronal genes. (A) Schematic showing the experimental strategy for *Lnc-Nr2f1* overexpression. In control mouse ES cells, an inverted construct with a splice acceptor (marked in yellow) and a polyadenylation signal (marked in red) is used. Overexpression of *Ngn2-Puro^R* with or without *Lnc-Nr2f1* or *Nr2f1* leads to induced neurons. Figure 3 continued on next page

Figure 3 continued

are added after the first exon of the *Inc-Nr2f1*. The mouse ES were infected with rtTA and Ngn2-T2A-puro and mES derived induced neurons (mES-iN) were assayed after 3 or 4 days after dox induction. (B) Graph showing that overexpression of *Inc-Nr2f1* increased the neurite length in day 3 Ngn2 mouse ES derived iN cells relative to the Ctrl. The same effect was not seen with *Nr2f1* overexpression. For each replicate, the individual neurite length for all neurons in each of the five 20x field was manually traced in Fiji. The sequence used for mouse *Inc-Nr2f1* overexpression is available in the supplementary document (n = 3, Student t-test, Two-tailed, * indicates $p=0.048 < 0.05$). Error bars show s.e.m. (C) Graph showing that overexpression of *Nr2f1* decreased the neurite number in day 3 Ngn2 mouse ES-iN cells relative to the Ctrl. The same effect was not seen with *Inc-Nr2f1* overexpression. (n = 3, 10 field per replicate, Student t-test, Two-tailed, ** indicates $p=0.0022 < 0.01$). Error bars show s.e.m. (D) β -III-tubulin staining of the day 3 Ngn2 mouse ES derived iN cells for Ctrl, *Inc-Nr2f1* overexpression and *Nr2f1* overexpression. Scale bar = 50 μ m. Red arrow pointed at immature induced neuronal cells with short projection. Green arrow pointed at mature induced neuronal cells with longer projection. Note that the *Inc-Nr2f1* overexpression condition have more mature induced neuronal cells. (E) Hierarchical clustering heatmap of day 4 Ngn2 ES-iN cells between control and *Inc-Nr2f1* overexpression (OE). There are 1912 genes differentially expressed (n = 2, FDR corrected $p < 0.10$, Fold change > 1.5 fold). Listed to the right are genes which are upregulated upon *Inc-Nr2f1* overexpression. (F) Schematic showing the knocking out strategy for *Inc-Nr2f1*. The *Inc-Nr2f1* knockout mouse ES cells are generated after Cre recombinase introduction to the Ctrl line in **Figure 3A**. The mouse ES were infected with rtTA and Ngn2-T2A-puro and mES derived induced neurons were assayed after 3 or 4 days after dox induction. (G) Hierarchical clustering heatmap of day 4 Ngn2 ES-iN cells between wild type, *Inc-Nr2f1* knockout (KO) and *Inc-Nr2f1* knockout with *Inc-Nr2f1* overexpression (OE). There are 348 genes differentially expressed and can be subsequently rescued with *Inc-Nr2f1* overexpression (n = 2, FDR corrected $p < 0.10$). Listed to the right are genes which are upregulated upon *Inc-Nr2f1* KO. (H) Gene ontology of the upregulated genes in *Inc-Nr2f1* knockout day 4 Ngn2 mouse ES- iN cells as compared to the Ctrl. (I) Gene ontology of the downregulated genes in *Inc-Nr2f1* knockout day 4 Ngn2 mouse ES- iN cells as compared to the Ctrl.

DOI: <https://doi.org/10.7554/eLife.41770.010>

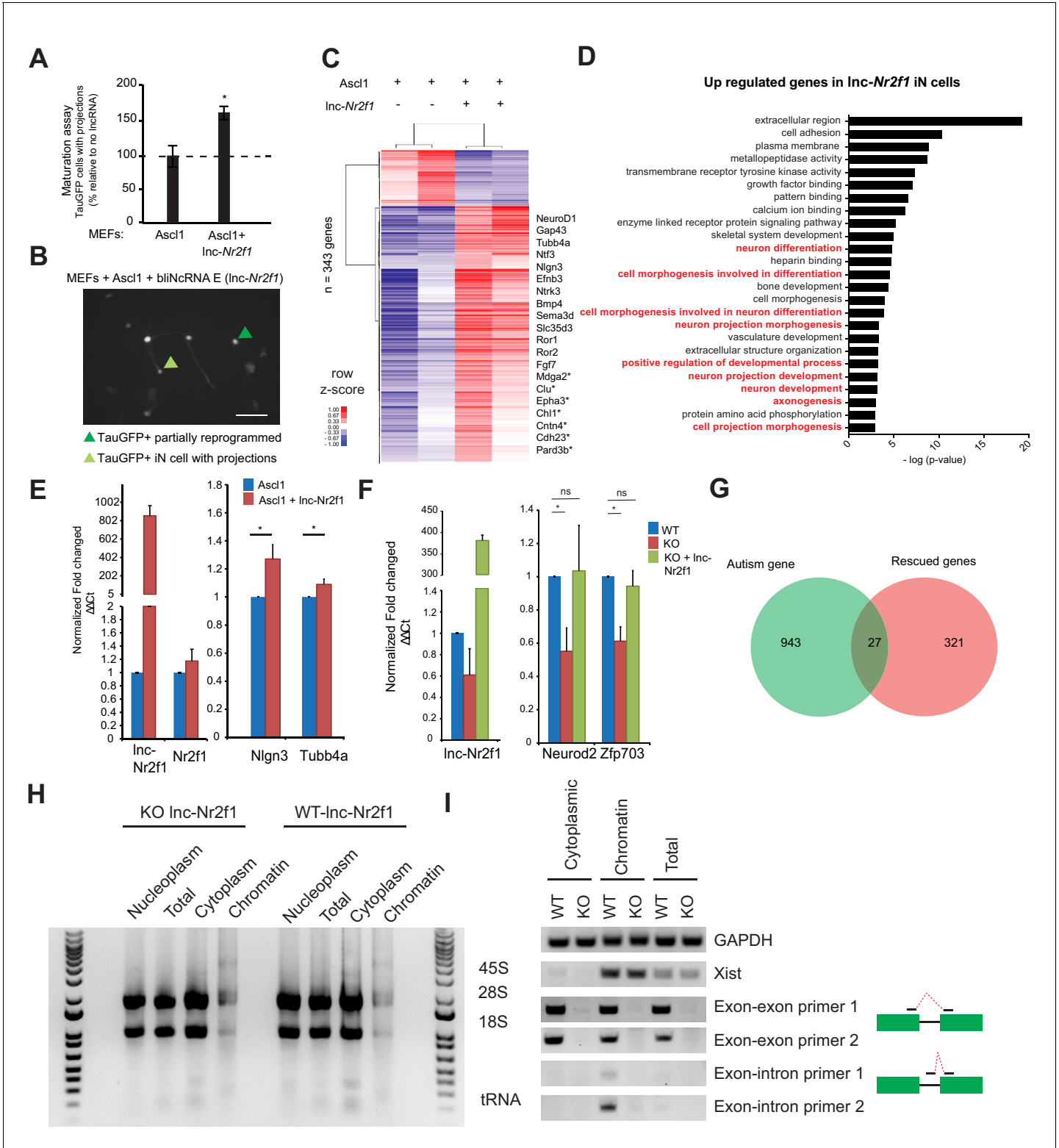


Figure 3—figure supplement 1. Characterization of the roles of *Inc-Nr2f1* during iN reprogramming. (A) Percentage of TauGFP positive cells with projections normalized to number of TauGFP cells. TauGFP cells with projections longer than three times the diameter of the cell body were counted and normalized to the total number of TauGFP positive cells. The sequence for mouse *Inc-Nr2f1* is available in the supplementary documents (n = 4, Student t-test, Two tailed, Error bars show s.e.m). (B) Immunofluorescence staining depicting how a TauGFP positive cell with projections (example highlighted in light green) is differentiated from a TauGFP positive partially reprogrammed iN cell (example highlighted in dark green) at 7 days. Scale Figure 3—figure supplement 1 continued on next page

Figure 3—figure supplement 1 continued

bar = 50 μ m. (C) Hierarchical clustering heatmap of differentially expressed genes detected by RNA-seq in MEFs expressing Ascl1 alone compared to Ascl1 and *Inc-Nr2f1* after 7 days ($n = 2$ biological replicates, FDR corrected $p < 0.001$). Shown are 343 genes. 311 genes are upregulated and 32 genes are downregulated. Fold change is represented in logarithmic scale normalized to the mean expression value of a gene across all samples. Representative gene names are included. Those with (*) have been linked to neurological disorders curated by Basu et al. (D) Gene ontology of the upregulated genes upon *Inc-Nr2f1* overexpression in Ascl1 MEF-iN 7 days. Highlighted in red are neuronal GO terms. (E) qRT-PCR validation downstream neuronal genes of the RNA-sequencing results in **Figure 1—figure supplement 3C**. Ectopic expression of *Inc-Nr2f1* led to upregulation of several downstream neuronal genes. ($n = 3$, * indicates $p < 0.05$). Error bars show s.e.m (F) qRT-PCR validation of several target genes in **Figure 3G** that go down when *Inc-Nr2f1* is knocked out which can be subsequently rescued with *Inc-Nr2f1*. ($n = 4$, * indicates $p < 0.05$). Error bars show s.e.m. (G) Venn diagram representing the overlap between autism related genes and rescued genes from **Figure 3G**. ($p = 0.0015$, $\chi^2 = 10.097$, $DF = 1$, Chi square test) (H) Non-denaturing TAE agarose gel showing the different species of RNA in different fractions. Note the presence of 45S in the chromatin fraction and tRNA and 5S in the cytoplasmic fraction. (I) RT-PCR performed on day4 mES iN using different primers targeting GAPDH (positive control), Xist (nuclear control), two independent exon-exon/exon-intron primers. WT and KO represent *Inc-Nr2f1* wild-type and knock-out mES-iN respectively.

DOI: <https://doi.org/10.7554/eLife.41770.011>

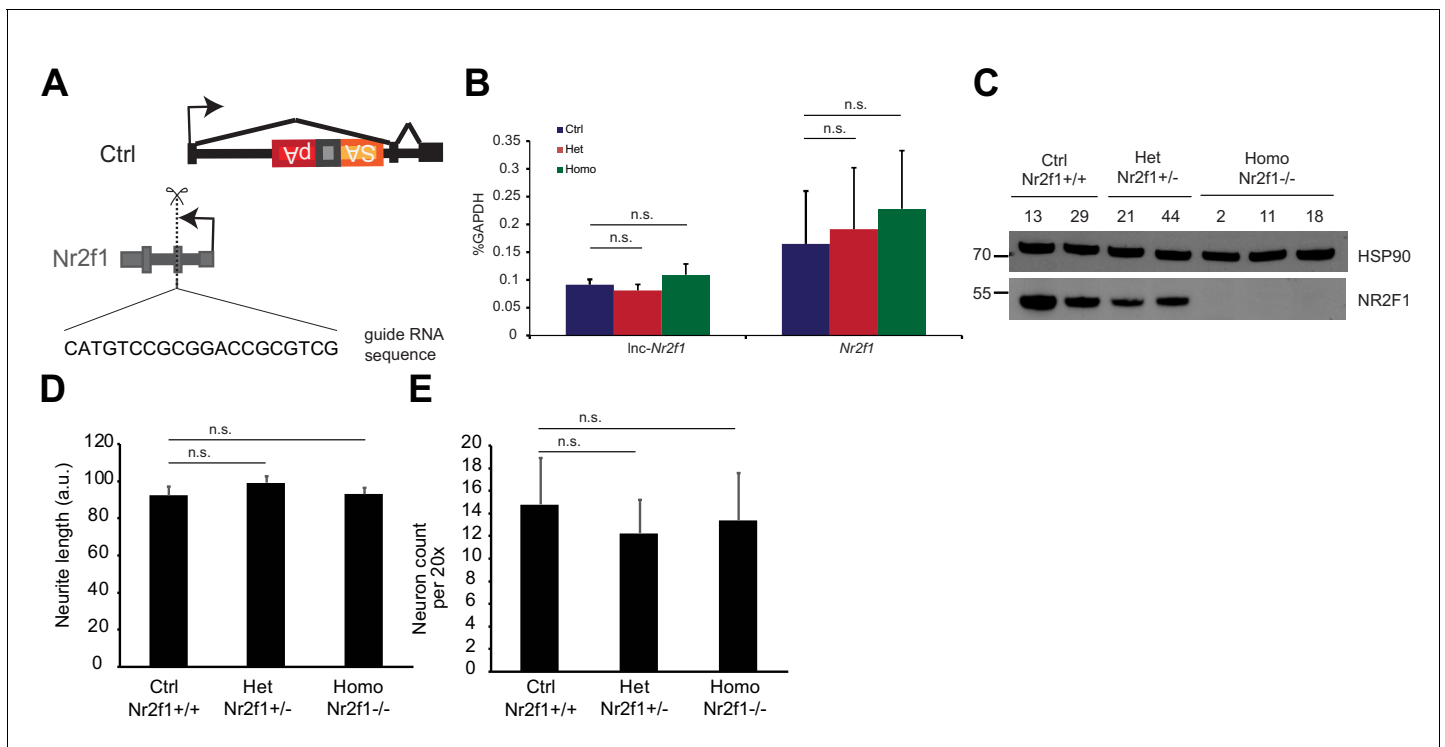


Figure 3—figure supplement 2. Characterization of the epistasis relationship between mouse *Nr2f1* and *Inc-Nr2f1*. (A) CRISPR knock out strategy to generate *Nr2f1* knockout (Homo) and heterozygous null lines (Het) from the control mES cells (Ctrl). (B) qRT-PCR results for *Inc-Nr2f1* and *Nr2f1* in the Ctrl, *Nr2f1* heterozygous null and *Nr2f1* knock out day 4 Ngn2 mES-iN. (n = 4 for Ctrl and Homo, n = 6 for Het; n.s. denotes not significant by two tailed t test) (C) Western blot showing the level of NR2F1 for individual clones of Ctrl, Het and Homo for day 4 Ngn2 mES-iN. (D) Neurite length measurement of the Ngn2 day 3 mES iN cells generated from the *Nr2f1* Ctrl, Het or Homo lines. (n = 4 for Ctrl and Homo, n = 6 for Het) (n.s. indicates p<0.05). (E) Number of neurons per 20x the Ngn2 day 3 mES iN cells generated from the *Nr2f1* Ctrl, Het or Homo lines. (n = 4 for Ctrl and Homo, n = 6 for Het) (n.s. indicates p<0.05).

DOI: <https://doi.org/10.7554/eLife.41770.012>

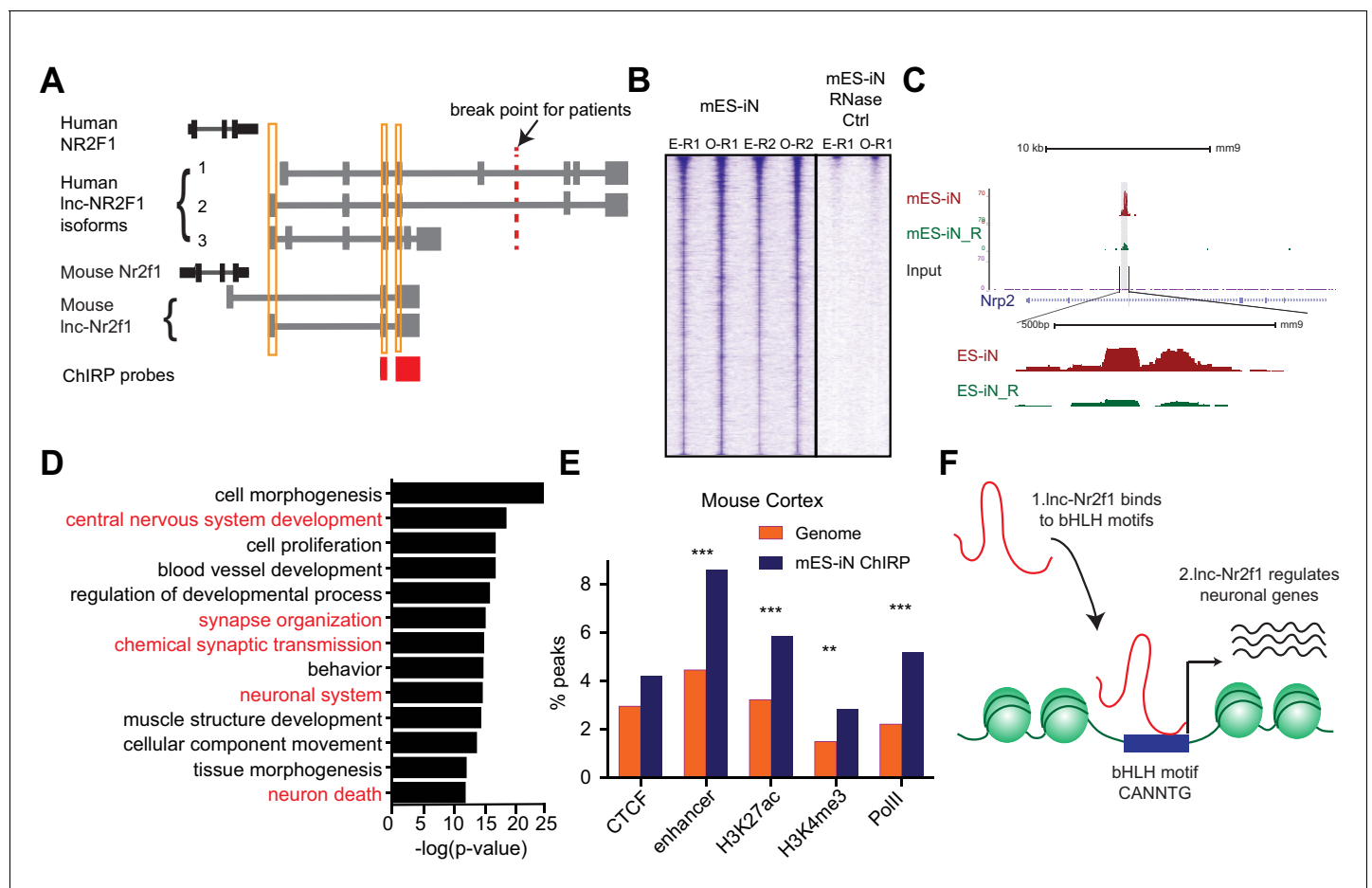


Figure 4. *Inc-Nr2f1* binds to distinct genomic loci regulating neuronal genes. (A) Schematic showing the location of ChIRP probe for mouse *Inc-Nr2f1* (highlighted in red). Yellow lines represent the conserved exons between mouse and human *Inc-Nr2f1*. (B) Heatmaps representing genome-wide occupancy profile for mouse *Inc-Nr2f1* in day 4 Ngn2 mouse ES-iN cells and the RNase control obtained by ChIRP. There are 14975 significant peaks called with respect to the RNase treated control. E and O represents even and odd probes respectively. (C) UCSC browser track showing the binding site within the intronic region of *Nrp2*. The 'R' represents the RNase treated control. (D) Gene ontology terms associated with genes adjacent to the high confident mES-iN ChIRP-seq peaks. Terms highlighted in red are terms related to nervous system development. (E) Percentage of mES-iN ChIRP-seq peaks which overlap with CTCF, enhancer, H3K27ac, H3K4Me3 and PolII defined in mouse cortex relative to the control. (***) represents $p < 0.0001$, ** represents $p < 0.01$, Chi-square test) (F) Proposal mechanism of *Inc-Nr2f1* action. *Inc-Nr2f1* binds to the genomic region enriched with bHLH motif and regulates the downstream neuronal genes.

DOI: <https://doi.org/10.7554/eLife.41770.013>

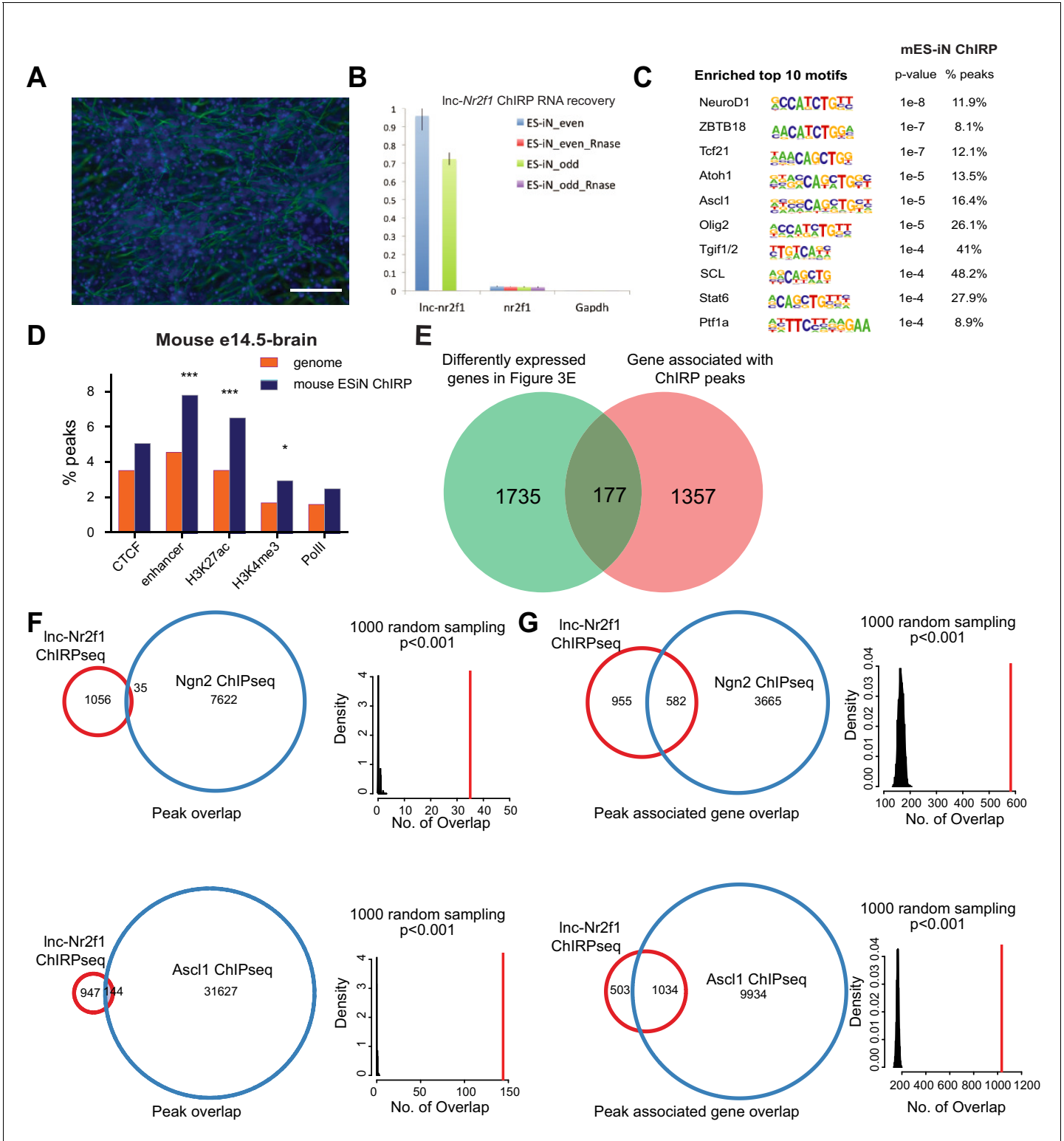


Figure 4—figure supplement 1. Identification of *Inc-NR2F1* role in transcriptional regulation. (A) Immunofluorescence staining for the day four mouse embryonic stem cell derived induced neurons (mES-iN) used in the *Inc-Nr2f1* ChIRP. (Green=β-III-tubulin, Blue = DAPI) (Scale bar = 50 μm) (B) *Inc-Nr2f1* RNA pull down efficiency for both even and odd probes (C) The enriched motifs with their corresponding p-value and the percentage of peaks with the given motifs. (D) Percentage of mES-iN ChIRP-seq peaks which overlap with CTCF, enhancer, H3K27ac, H3K4Me3 and PolII defined in mouse E14.5 brain relative to the control. (***) represents $p < 0.0001$, * represents $p < 0.05$, Chi-square test) (E) Venn diagram showing the overlap between 1912 genes from **Figure 3E**, and the 1534 genes adjacent to the 1092 high confident mES-iN ChIRP peaks. ($p < 0.0001$, $\chi^2 = 21.983$, DF = 1, Chi square test)

Figure 4—figure supplement 1 continued on next page

Figure 4—figure supplement 1 continued

(F) Venn diagram and statistical analysis of the overlapped peaks between lnc-Nr2f1 ChIP-seq peaks and Ngn2 (top) or Ascl1 (bottom) ChIP-seq peaks. Right panels are the null distribution of overlapped peaks constructed by 1000 random sampling. The number of overlap peaks in the observed data is marked in solid red line. (G) Venn diagram and statistical analysis of the overlapped peak-associated-genes between lnc-Nr2f1 ChIP-seq and Ngn2 (top) or Ascl1 (bottom) ChIP-seq. Right panels are the null distribution of overlapped genes constructed by 1000 random sampling. The number of overlap genes in the observed data is marked in solid red line.

DOI: <https://doi.org/10.7554/eLife.41770.014>

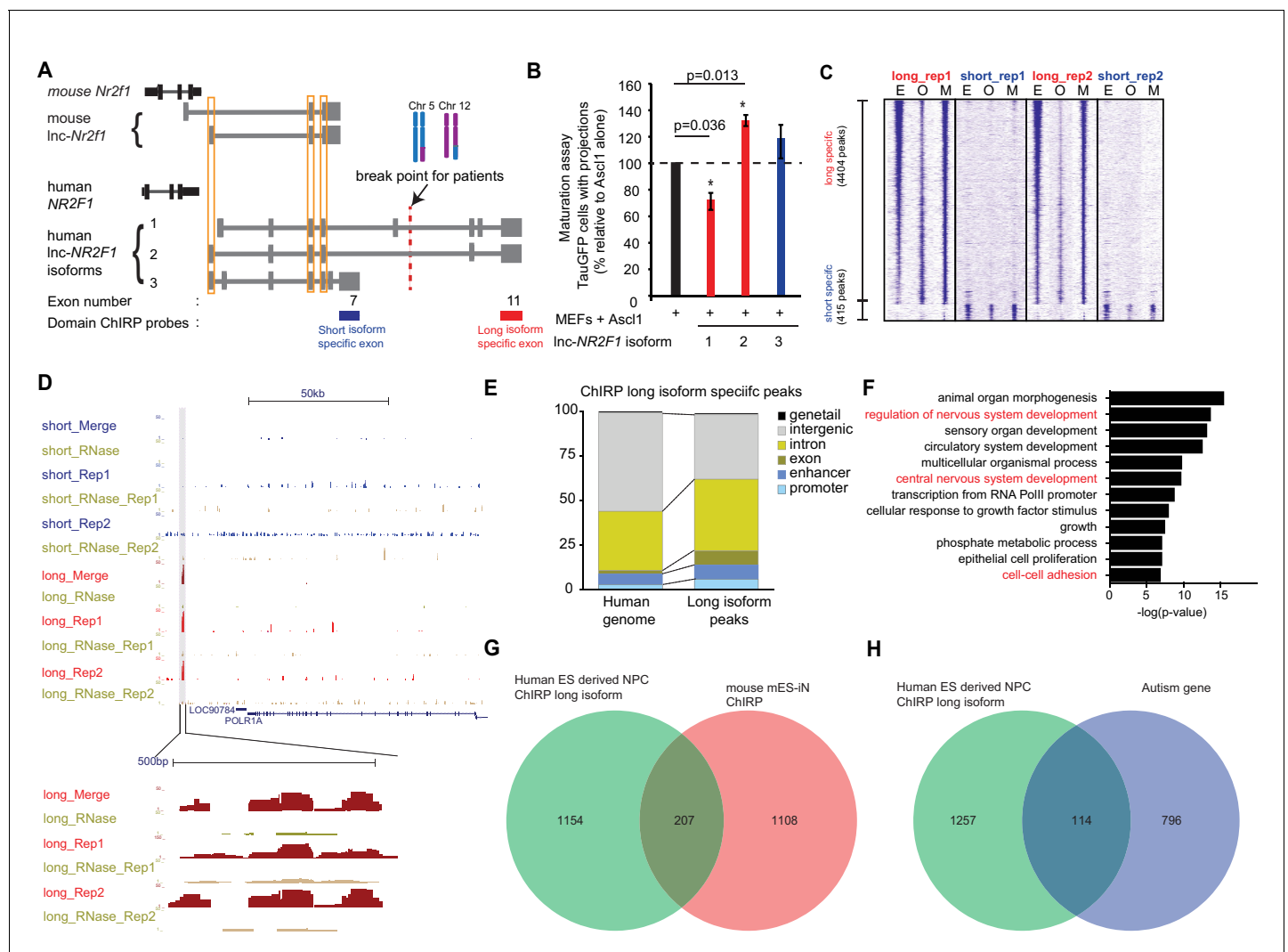


Figure 5. Human *Inc-NR2F1* shows isoform-specific chromatin binding. (A) Schematic showing the location of the ChIP probes target the short isoform-specific exon (exon 7) and long isoform-specific exon (exon 11). The red line denotes the break point for the patient. (B) Overexpression of human *Inc-NR2F1* isoforms in combination with Ascl1 relative to MEFs expressing Ascl1 alone. The graph quantifies the proportion of TauGFP positive cells with projections normalized to number of TauGFP cells. TauGFP cells with projections longer than three times the diameter of the cell body were counted and normalized to the total number of TauGFP positive cells. The sequences for human *Inc-Nr2f1* isoforms is available in the supplementary documents (n = 3, Student t-test, two tailed, scale bar = * represents $p < 0.05$, ** represents $p < 0.01$). Error bars show s.e.m. (C) Heatmap representing genome-wide occupancy profile for domain ChIP performed using probes specific to the long and short isoform-specific exon of *Inc-NR2F1* in human ES derived neural progenitor cells (NPC). There are 4404 and 415 significant peaks called relative to the RNase control for the long and short isoform respectively. E, O and M represents even, odd and merge track respectively. (D) UCSC browser track showing the site within the promoter region of LOC90784 bound by the long isoform-specific exon (exon 11) but not the short isoform-specific exon (exon 7) (E) Bar graph showing the distribution of the 913 high confident long isoform-specific peaks. The long isoform-specific peaks are enriched in the introns, exons, promoters and enhancers but depleted in the intergenic regions. (F) Gene ontology terms associated with genes adjacent to the human ES derived NPC ChIP-seq high confident peaks. Terms highlighted in red are terms related to nervous system development. (G) Venn diagram representing the peak associated gene overlap between the domain ChIP of the long isoform-specific exon (exon 11) from human ES derived NPC and mouse mES-iN ChIP. ($p < 0.0001$, $\chi^2 = 239.921$, DF = 1, Chi square test) (H) Venn diagram representing overlap between genes involved in the autism risk and genes identified by the domain ChIP of the long isoform-specific exon (exon 11) from human ES derived NPC. ($p < 0.0001$, $\chi^2 = 71.670$, DF = 1, Chi square test).

DOI: <https://doi.org/10.7554/eLife.41770.015>

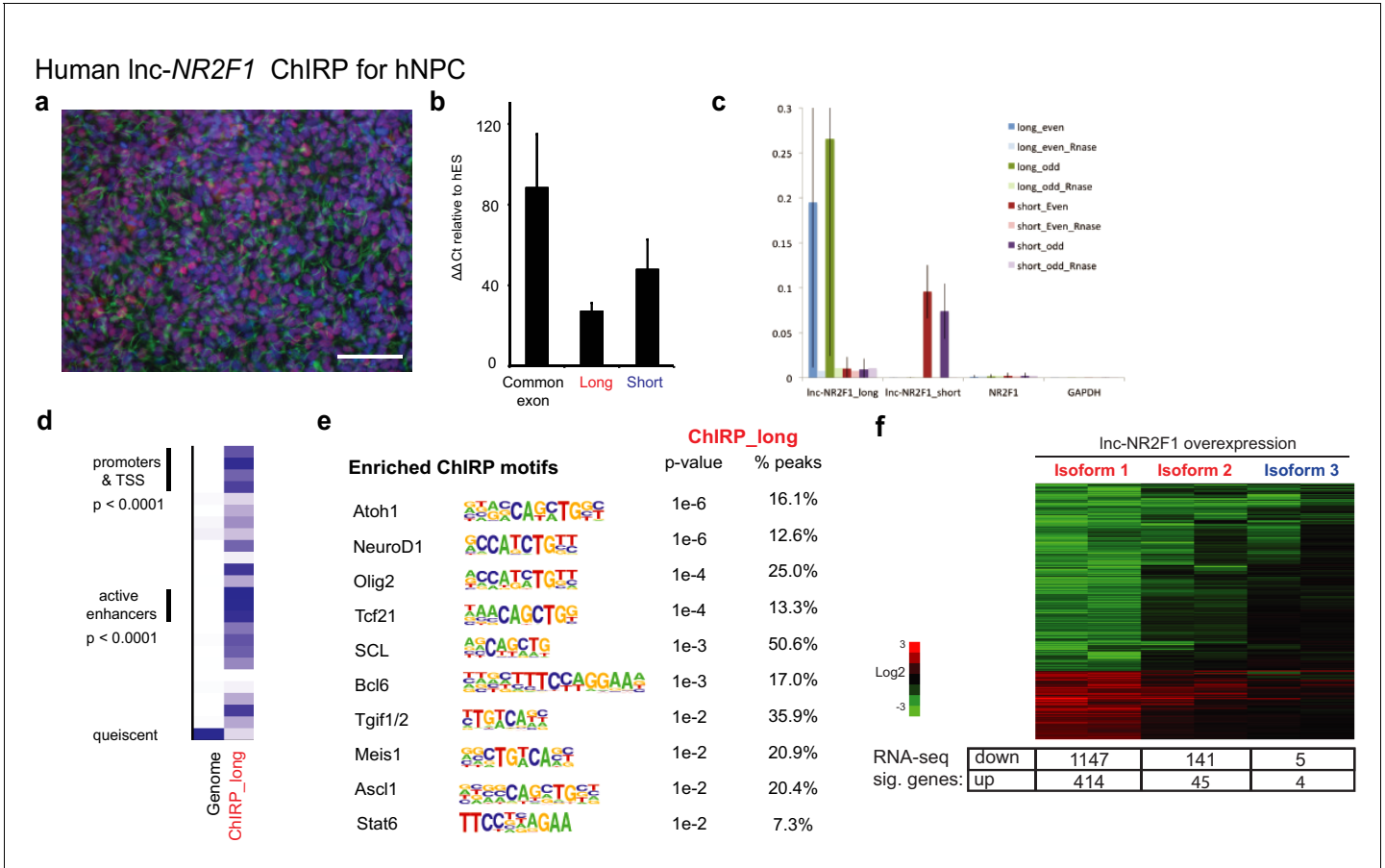


Figure 5—figure supplement 1. Identification of *lnc-NR2F1* role in transcriptional regulation. (A) Immunofluorescence staining for day 12 human neural progenitor cells (hNPC) differentiated from H9 cells using dual SMAD protocol. (Green = human NESTIN, Red = human SOX1, Blue = DAPI) (Scale bar = 50 μ m) (B) qRT-PCT using primers specific to the common, long or short exon in day 12 hNPC. (n = 3). (C) *lnc-NR2F1* RNA pull down efficiency for the long and short isoform-specific exons of for both even and odd probes. The pull down is specific to *lnc-NR2F1* since there is very little *NR2F1* or *GAPDH*. (D) ChromHMM model ran on the peaks from the high confident long isoform-specific exon (exon 11) ChIRP peaks performed in hNPC. The peaks are enriched in the promoters and TSSs, active enhancers and quiescent chromatin regions. (E) The enriched transcription factor motifs for the long isoform-specific domain ChIRP experiments in hNPC. (F) Heatmap showing the gene expression changes in a human neuroblastoma cell line (SK-N-SH) upon overexpression of human *lnc-NR2F1* isoform 1, 2 and 3 respectively normalized to the control (>2 fold, p<0.05, FDR < 0.05). The box below the heatmap shows the number of genes significantly upregulated or downregulated.
DOI: <https://doi.org/10.7554/eLife.41770.016>